BACKGROUND SEGMENTATION IN MICROSCOPY IMAGES

J.J. Charles, L.I. Kuncheva
School of Computer Science, University of Wales, Bangor, LL57 1UT, United Kingdom
jjc@informatics.bangor.ac.uk

B. Wells
Conwy Valley Systems Ltd, United Kingdom

I.S. Lim
School of Computer Science, University of Wales, Bangor, LL57 1UT, United Kingdom

Keywords: Image processing, image analysis, segmentation, background removal, microscope, vignetting, microfossils, kerogen, palynofacies, palynomorphs

Abstract: In many applications it is necessary to segment the foreground of an image from the background. However images from microscope slides illuminated using transmitted light have uneven background light levels. The non-uniform illumination makes segmentation difficult. We propose to fit a set of parabolas in order to segment the image into background and foreground. Parabolas are fitted separately on horizontal and vertical stripes of the grey level intensity image. A pixel is labelled as background or foreground based on the two corresponding parabolas. The proposed method outperforms the following four standard segmentation techniques, (1) thresholding determined manually or by fitting a mixture of Gaussians, (2) clustering in the RGB space, (3) fitting a two-argument quadratic function on the whole image and (4) using the morphological closure method.

1 INTRODUCTION

Images with non-uniform background illumination appear in various applications, e.g., in biology, medicine, astronomy and geology. Most cases of uneven illumination occur when taking images through a microscope or telescope. The periphery of the image is usually poorly illuminated and this is known as vignetting. There are three main types of vignetting, mechanical, optical and pixel. Mechanical vignetting is caused by the physical construction of the optical viewing device while optical vignetting is inherent in the lens design. Pixel vignetting only occurs in digital cameras due to less light hitting a photon cell at an oblique angle, i.e., towards the edges of the image.

The microscopy images of interest in this study come from rock and drill cuttings and contain microfossils and other organic debris on a light background. The images are taken with transmitted light microscopy. The concentrated light source compounds the effect of vignetting causing even worse illumination across the image. The background is typically brighter in the middle and darker towards the edges.

The most common method to segment the foreground from the background of an image is thresholding (Otsu, 1979; Cinque et al., 2004; Sankur and Sezigin, 2004). However, using a constant threshold will result in objects of interest near the edges of the image being lost within a "rim" labelled as foreground. On the other hand, light objects in the middle of the image will be blended with the background. In this case global thresholding will have to be replaced with local thresholding. To perform local thresholding a background estimate is required so that an individual threshold is set for each pixel. A common method for obtaining this estimate is to use the image of an empty microscope slide as a template. However a single estimate may not be suitable for all images due to possible changes in the microscope setup. This is why we seek a method for unique background estimation based solely on the image provided. It has been shown that as the light intensity fades with the square of the distance from the source, a quadratic function can be used to model the illumination (Montage, 2002). Higher order surface polynomials have also been used but, typically these are applied to images captured using techniques where vignetting is not the cause of uneven illumination (Zawada, 2003). These single-function models may be too coarse and

inaccurate, especially when the foreground occupies a substantial part of the image. The distortion in illumination from a lens system has shown to be described by the 4th power of a cosine function (Asada et al., 1996), it is this that inspired Zawada (Yu et al., 2004) to estimate the illumination using a hyperbolic function. Other methods include convolving the image with a Gaussian kernel (Leong et al., 2003). The idea is to smooth the image until it is devoid of features but retains the average intensity across the image. This technique is unautomated and will need the assistance of a human controller to set parameters and make corrections within graphics editing software.

2 BACKGROUND REMOVAL BY FITTING HORIZONTAL AND VERTICAL PARABOLAS

As explained above, a quadratic function can be used to model the illumination in an image

$$f(x,y) = A + Bx + Cy + Dx^2 + Ey^2 + Fxy, \qquad (1)$$

where x and y are the pixel's coordinates, and $f(x,y)$ approximates the grey level intensity of the background at (x,y). Although theoretically sound, this model may be too coarse for the purposes of the background/foreground segmentation. Instead of fitting a two-argument quadratic function, we propose to fit multiple "horizontal" and "vertical" parabolas.

The proposed method consists of the following steps:

(i) The grey level intensity image is split into K_y vertical and K_x horizontal stripes. An example of a horizontal stripe of a microscopy image containing microfossils is shown in Figure 1. The intensities on each stripe are averaged across the smaller dimension of the stripe so that a single mean line is obtained.

(ii) A parabola is fitted on each mean line using an iterative procedure similar to that for removing background from spectra. Consider horizontal stripe i. Denote the intensities on the mean line of the stripe by $g_i(x)$, where x spans the width of the image. Using least squares, fit a parabola $z_i^{(1)}(x) = a_i + b_i x + c_i x^2$ to approximate $g_i(x)$. As the mean line includes intensities of both background and foreground pixels, $z_i^{(1)}(x)$ will not model the background only. Figure 2 shows the mean line for the stripe from Figure 1. Plotted with the dot marker is $z_i^{(1)}(x)$.

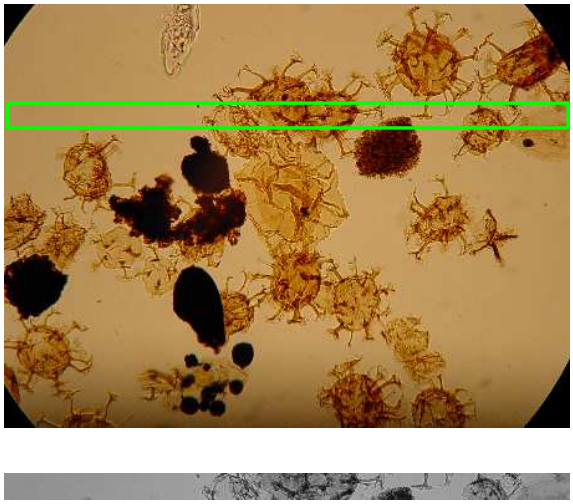

Figure 1: The original image of palynofacies and a grey stripe cut along the x-axis

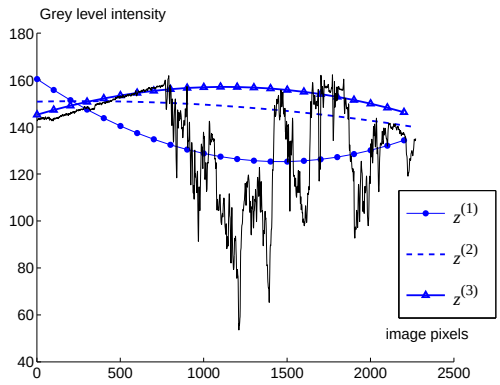

Figure 2: Grey level intensity of the mean line and the three subsequently fitted parabolas for the stripe in Figure 1

To exclude the foreground points, a second parabola is fitted, denoted $z_i^{(2)}(x)$, using a reduced set of points on the mean line $\left\{x \,\middle|\, g_i(x) > z_i^{(1)}(x)\right\}$. By requiring that the grey level intensity exceeds $z_i^{(1)}(x)$, the most "certain" foreground pixels are eliminated from the approximation. The resultant parabola $z_i^{(2)}(x)$ is shown in Figure 2 with a dashed line. A third iteration is carried out in the same way, this time using the set $\left\{x \,\middle|\, g_i(x) > z_i^{(2)}(x)\right\}$ to derive $z_i^{(3)}(x)$ (triangle maker in Figure 2). It was found empirically that three iterations give a sufficiently good result.

(iii) Consider pixel (x,y) with grey level intensity $p(x,y)$. Let the pixel be in the i-th horizontal stripe and j-th vertical stripe. The pixel is labelled as

foreground (object) iff

$$p(x,y) < \left\{ z_i^{(3)}(x) - T_i,\ z_j^{(3)}(x) - T_j \right\}, \qquad (2)$$

where T_i and T_j are automatically calculated thresholds as explained later. Otherwise the pixel is labelled as background. In other words, the point must be classed as foreground in **both** horizontal and vertical directions in order to receive a final label as foreground. The segmented image is obtained by labelling all pixels in the image in this way.

3 EXPLANATION OF THE METHODOLOGICAL AND PARAMETER CHOICES

I. The choice of two one-dimensional models instead of a joint quadratic model was based on empirical observation. The segmentation accuracy of the joint quadratic model appeared to be compromised for some images, arguably because of the coarse approximation.

II. The decision to divide the image into stripes was dictated by the large computational demand should each horizontal and vertical line be processed in turn. We found empirically that $K_x = \text{ceiling}(\text{No. Rows}/40)$ and $K_y = \text{ceiling}(\text{No. Columns}/40)$ is a good compromise between accuracy and speed.

III. The need to combine the horizontal and vertical labelling with an "and" operation (equivalent to making the decision by equation (2)) is explained below. Some images contain a large proportion of objects located at the centre. This may cause the parabola to be a trough rather than a hill even after the third iteration ($z_i^{(3)}(x)$). Then the edges of the image will be mislabelled as foreground. It is unlikely that the same will happen to the orthogonal stripe that runs across that edge. If a pixel is labelled as background in that stripe, the overall label assigned by (2)) will be corrected to "background". Figure 3 shows the results from applying separately a horizontal and a vertical approximation. Unwanted artefacts in the form of skidmarks are present in both images. Only when a point is labelled as foreground in both images its overall label will be returned as "foreground".

IV. The thresholds T_i and T_j are determined automatically from the respective parabolas $z_i^{(3)}(x)$ and $z_j^{(3)}(x)$. The parabola gives the "middle" background intensity in the stripe. However, fluctuations about the curve may also belong in the background. The following heuristic threshold T_i is proposed for horizontal stripe i

$$T_i = \max_x z_i^{(3)}(x) - \text{mean}_x z_i^{(3)}(x) \qquad (3)$$

T_j is calculated in the same way for the vertical stripes. Using the standard deviation of the points or the maximum residual are additional possibilities for constructing the thresholds.

4 EXPERIMENTS

The background removal method was applied to a variety of microscopy images of microfossils. This technique takes less than 0.8 s for an image of 758 by 568 pixels when run using Matlab on a PC with a Pentium-4 3.2-GHz processor and 2GB of RAM. The following *alternative* segmentation methods were also tried

1. Thresholding the image with a manually adjusted constant threshold. Only visual feedback was used to tune the threshold.
2. Fitting a mixture of two Gaussians on the grey level histogram and finding the intensity corresponding to the minimum-error classification between class "background" and "other". This intensity was used as a threshold across the whole image. Three Gaussians were also attempted because the images of interest contain darker and lighter objects (two foreground classes) and the background, as seen in Figure 1. Figure 4 illustrates this technique. The three fitted Gaussians are overlaid on the grey level histogram of the image and the threshold (138) is marked with a large dot. (The thresholds found when two Gaussians were fitted was 137.)

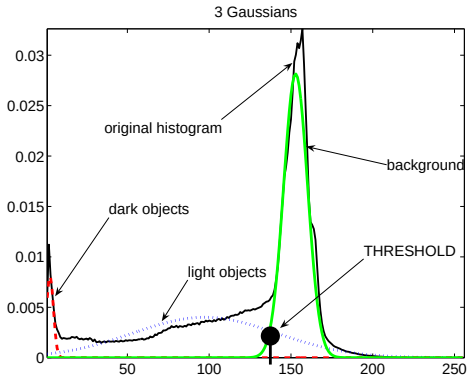

Figure 4: The grey level histogram of the image in Figure 1 and the fitted mixture of three Gaussians. The threshold is marked with a large dot.

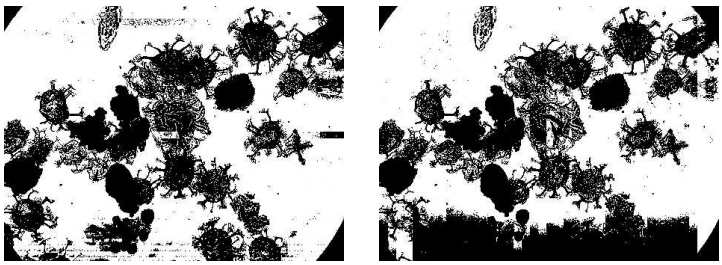

Horizontal scan Vertical scan

Figure 3: Results from applying separately a horizontal and a vertical approximation

3. Subtracting the morphological closing of the image from the original and performing a manual threshold on the result (Gonzalez et al., 2004). The closing of a greyscale image will suppress dark regions, masking over the foreground pixels with intensities of local background pixels. By subtracting this from the orignal greyscale image we hope to produce an image of even illumination, thus allowing a global threshold to be applied. The exact operation of this procedure is decided by a structuring element. The size of this structuring element will determine which dark regions are masked.

4. Clustering in the original RGB space. Figure 5 shows an example of the results of applying k-means clustering to a random sample of 150 pixels from the image in Figure 1. Three clusters were identified, corresponding to background, light and dark objects, and their projection onto the axes "red" and "green" are displayed. The covariance matrices of the clusters were estimated and the pixels in the original image were then labelled into foreground and background using the Mahalanobis distances to the cluster centres. No improvement was found when using a larger sample of pixels.

5. Fitting a quadratic function. As in the proposed method, three functions were fitted in the same iterative way in order to eliminate the effect of foreground pixels on the approximation.

6. Fitting a B-spline surface. Lindblad and Bengtsson (Lindblad and Bengtsson, 2001) propose to fit a B-spline surface using a least squares estimate to correct the light intensity across the image. A global threshold is then applied to segment background from foreground pixels. In this example we calculated the threshold as in method 3 (fitting three Gaussians).

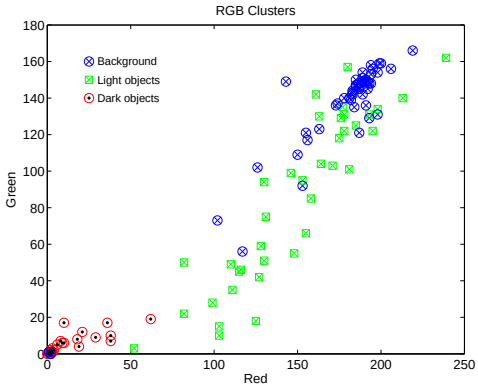

Figure 5: Three clusters of pixels in the RGB space, projected onto the R-G axes.

The accuracy of the results was evaluated visually across a collection of images. Figure 7 gives a typical example of the segmentation results through methods 1 to 6, the proposed method is show in figure 8. Out of the six alternative methods, method 6 showed the best results. Methods 3 and 5 showed some missing or partly captured semi-transparent objects corresponding to organic material. These objects are highlighted by ellipses and circles in Figure 7. The proposed technique and method 6 extracted these objects much more adequately.

Given underneath each subplot is the average computational time from 3 runs of the chosen method on the same image. The small changes in processing time for each run was attributed to background tasks in Windows XP operating system. (The standard deviations of the processing times were negligible.) The computational times indicate that the proposed method offers a good trade-off between accuracy and speed compared to the alternatives examined in this study.

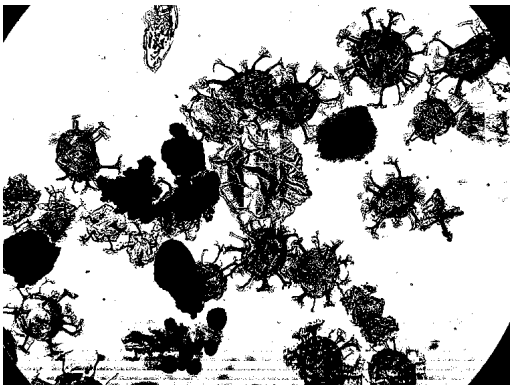

Figure 8: **(6) PROPOSED: Parabola fit (0.7787s)**

The accuracy of method 6 closely matches that of the proposed method, however we have found that in certain circumstances the proposed technique is better than method 6. We generated 10 non-uniform backgrounds of size 200 by 200 pixels. For each background a dark ring was placed in the centre as a foreground object. The proposed technique and the B-spline method were both used to segment the ring from the image. The accuracy was estimated by calculating the number of pixels misclassified by the methods.

Ten rings of constant thickness (30 pixels) with increasing inner radius were created and placed one at a time in the centre of the background. The inner radii of the circles, expressed as a percentage of the image width, were 5%, 10%, ..., 50%. For images with inner radius less than 5% to 40%, the proposed method was better than the B-spline method while at radii 45% and 50% the B-spline method was better.

Figure 6 demonstrates why the proposed method works better than the B-spline method. Subplot (a) shows the generated image with a dark ring. Subplot (b) shows only the generated background. Subplot (c) shows the estimated background using B-spline. The proposed method can also estimate the background of the generated image; this is shown in subplot (d). Notice that the foreground has pulled the background estimate of method 6 towards lower intensity values however the proposed method ignores these low intensity values creating an adequate background estimate.

5 CONCLUSIONS

A segmentation method is proposed which models uneven background in microscopy images by a set of horizontal and vertical parabolas. The method outperforms five standard segmentation techniques on a collection of test images at a competitive computational speed. This approach is an automated one as apposed to morphological closing that requires manually selecting a structuring element.

The number of parameters that are tuned for the proposed method far exceeds those of the standard methods and this is why a better segmentation is found. Manual thresholding requires only 1 parameter. Fitting three gaussians each with a centre and standard deviation requires 6 parameters. Fitting a quadratic function entails tuning 6 parameters for the coefficients of the function. Clustering in RGB space uses 27 parameters, each of the three clusters has a centre in three dimensions and an associated covariance matrix. The covariance matrix contains 9 values but due to the symmetry only 6 of these are independent. The B-spline method uses a mesh of size 5x5 as the control points for the surface, hence 25 parameters are used. The proposed method uses 3 coefficients of a parabola fitted to each mean row and column. In our example we used 15 parabolas for the horizontal fit and 19 for the vertical fit, which results in 102 parameters.

The segmentation offered by the B-spline method is in most cases as accurate as the one obtained by the proposed method. However, the proposed method takes a fraction of the time the B-spline method needs.

ACKNOWLEDGEMENTS

The EPSRC CASE grant Number CASE/CNA/05/18 is acknowledged with gratitude.

REFERENCES

Asada, N., Amano, A., and Baba, M. (1996). Photometric calibration of zoom lens systems. *IEEE International Conference on Patter Recognition*, pages 186–190.

Cinque, L., Foresti, G., and Lombardi, L. (2004). A clustering fuzzy approach for image segmentation. *Pattern Recognition*, 37(9):1797–1807.

Gonzalez, R. C., Woods, R. E., and Eddins, S. L. (2004). *Digital Image Processing Using Matlab*. Pearson Education, Inc.

Leong, F., Brady, M., and McGee, J. (2003). Correction of uneven illumination (vignetting) in digital microscopy images. *Journal of Clinical Pathology*, 56(8):619–621.

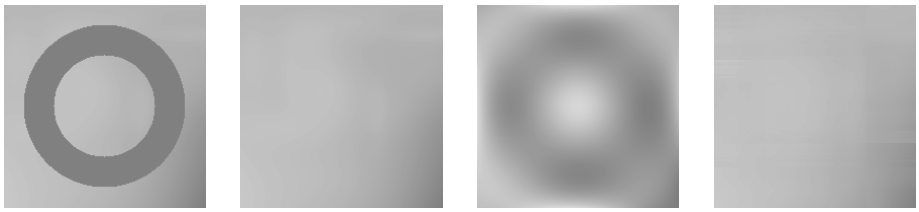

a b c d

Figure 6: (a) Generated image. (b) The true background. (c) The background estimated by the B-spline method. (d) The background estimated by the proposed method.

Lindblad, J. and Bengtsson, E. (2001). A comparison of methods for estimation of intensity nonuniformities in 2d and 3d microscope images of fluorescence stained cells. *Proceedings of the 12th Scandinavian Conference on Image Analysis (SCIA)*, pages 264–271.

Montage (2002). Baseline background correction. `http://montage.ipac.caltech.edu/baseline.html`.

Otsu, N. (1979). A threshold selection method from gray level histogram. *IEEE Trans. Systems, Man and Cybernetics*, 9:62–66.

Sankur, B. and Sezigin, M. (2004). Survey over image thresholding techniques and quantitative performance evaluation. *Journal of Electronic Imaging*, 13(1):146–165.

Yu, W., Chung, Y., and Soh, J. (2004). Vignetting distortion correction method for high quality digital imaging. *17th International Conference on Pattern Recognition*, 3:666–669.

Zawada, D. G. (2003). Image processing of underwater multispectral imagery. *IEEE Journal of Oceanic Engineering*, 28(4):583–594.

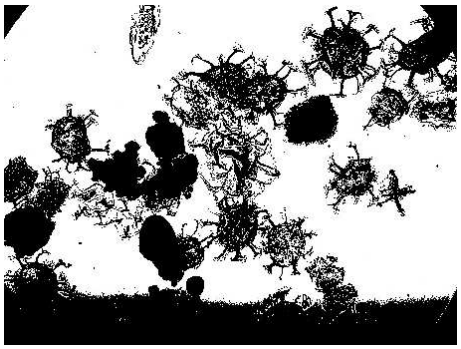

(1) Manual thresholding (thr = 135)

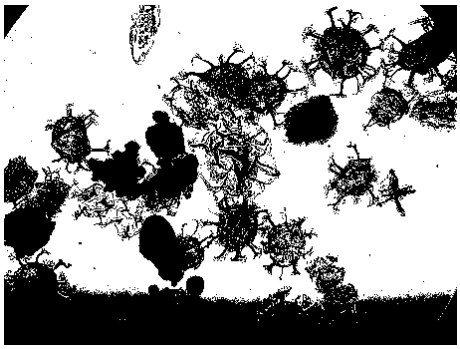

(2) 3 Gaussians fitted (thr = 138)
(2.6474 s)

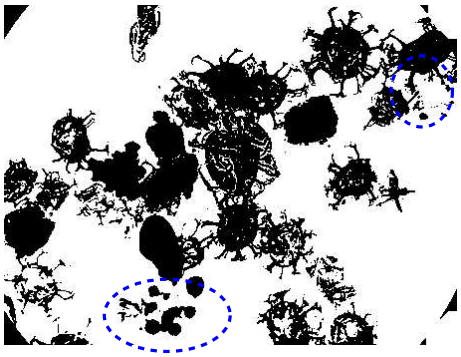

(3) Morphological closing
(1.4267 s)

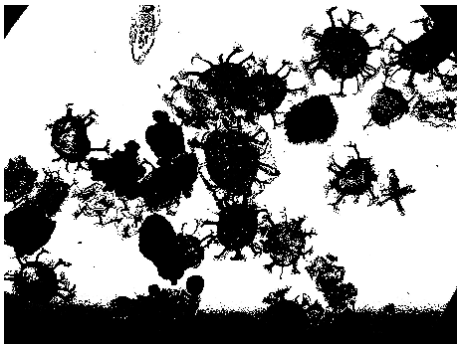

(4) Clustering in RGB (3 clusters)
(0.8706 s)

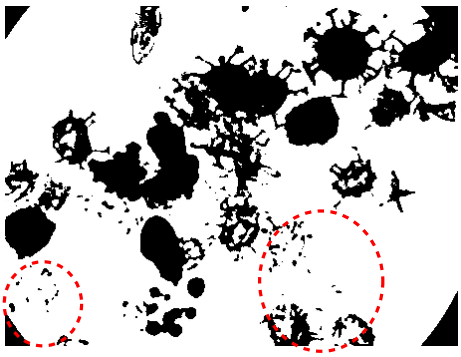

(5) Joint quadratic surface
(0.2938s)

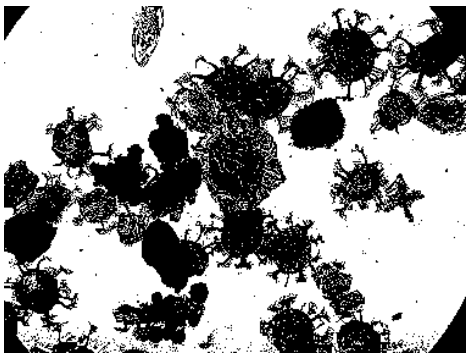

(6) B-spline method
(32.2186 s)

Figure 7: Experimental results: Background removal with the proposed method and the 5 alternative methods